

# Transient Growth and Optimal Excitation of Thermohaline Variability

ELI TZIPERMAN

*Environmental Sciences, Weizmann Institute, Rehovot, Israel*

PETROS J. IOANNOU

*Faculty of Physics, University of Athens, Athens, Greece*

(Manuscript received 1 October 2001, in final form 20 May 2002)

## ABSTRACT

The physical mechanisms of transient amplification of initial perturbations to the thermohaline circulation (THC), and of the optimal stochastic forcing of THC variability, are discussed using a simple meridional box model. Two distinct mechanisms of transient amplification are found. One such mechanism, with a transient amplification timescale of a couple of years, involves an interaction between the THC induced by rapidly decaying sea surface temperature anomalies and the THC induced by the slower-decaying salinity mode. The second mechanism of transient amplification involves an interaction between different slowly decaying salinity modes and has a typical growth timescale of decades. The optimal stochastic atmospheric forcing of heat and freshwater fluxes are calculated as well. It is shown that the optimal forcing induces low-frequency THC variability by exciting the salinity-dominated variability modes of the THC.

## 1. Introduction

Quite a few physical mechanisms of thermohaline circulation (THC) variability have been proposed over the past few years, varying from damped linear oscillations excited by stochastic atmospheric forcing (e.g., Griffies and Tziperman 1995), interpreting the coupled GCM study of Delworth et al. (1993) via self-sustained small amplitude variability (e.g., Chen and Ghil 1995), jumps between different equilibria induced by stochastic forcing (Cessi 1994), to larger self-sustained amplitude variability (e.g., Weaver et al. 1991), and to yet stronger THC flushes (e.g., Winton and Sarachik 1993). Present-day THC variability is most likely of a fairly small amplitude (5%–10% of the mean value), so that linearized dynamics might be able to describe it relatively well. It is known that stable non-normal linear systems can undergo large transient amplification given optimal perturbations (Farrell 1988; Farrell and Ioannou 1996). One wonders whether such transient amplification is also relevant to the dynamics of present-day THC variability.

The nonnormal nature of the THC dynamics could play a role in two different contexts that motivate the present work. First, optimal initial conditions could result in large transient THC amplification. While the

THC seems to have been quite stable for about 10 000 years, there are indications that it might be close to an instability threshold (Tziperman et al. 1994; Tziperman 1997) below which the THC may become unstable. Are there transient amplification mechanisms that may result in a transition of the climate system to below the THC stability threshold? The second question to be studied here is whether a continuous excitation of the nonnormal dynamics by atmospheric noise could result in a significant THC variability, and what might be the physical mechanism behind the optimal stochastic forcing. We study these issues in the framework of a simple box model that is described in section 2. The results for the optimal initial conditions and mechanisms of transient THC growth are described in section 3 and those for the optimal stochastic forcing are described in section 4. We conclude in section 5.

## 2. The model

The model (Fig. 1) is chosen to be the simplest THC meridional box model that displays the oscillatory THC mode studied by Tziperman et al. (1994) and Griffies and Tziperman (1995). There are three ocean boxes, with box 1 representing the midlatitude upper ocean, box number 2 representing the polar ocean, and box 3 the midlatitude deep ocean. The model equations are

---

Corresponding author address: Dr. Eli Tziperman, Environmental Sciences, Weizmann Institute, Rehovot 76100, Israel.  
E-mail: eli@beach.weizmann.ac.il

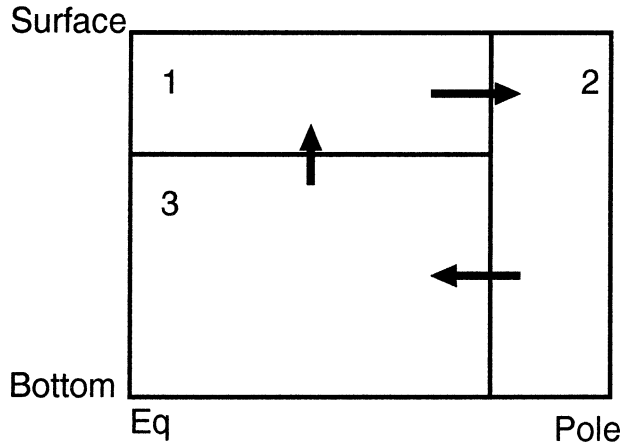


FIG. 1. The meridional THC box model.

$$\begin{aligned}
 U &= u_0 \{ \rho_2 - [\delta \rho_1 + (1 - \delta) \rho_3] \} \\
 \rho &= -\alpha T + \beta S \\
 \dot{T}_1 &= U(T_3 - T_1)/V_1 + \gamma(T_1^* - T_1) \\
 \dot{S}_1 &= U(S_3 - S_1)/V_1 + FW_1/V_1, \quad (1)
 \end{aligned}$$

with the above temperature and salinity equations written for the case of a thermally dominant mode ( $U > 0$ ). The equations for the two other boxes and for negative (salinity dominant) THC are written using the same standard box model upwind differencing scheme (Rivlin and Tziperman 1997). The north-south dimensions of the boxes are  $L_{1,2,3} = 5000, 2000, 5000$  km; their depths  $H_{1,2,3} = 1, 5, 4$  km; and their width  $W = 4000$  km. The model parameters are  $u_0 = 16/0.0004$  Sv g cm $^{-3}$  (1 Sv  $\equiv 10^6$  m $^3$  s $^{-1}$ ),  $\alpha = 1668 \times 10^{-7}$  g cm $^{-3}$  K $^{-1}$ ,  $\beta = 0.781 \times 10^{-3}$  g cm $^{-3}$  psu $^{-1}$ ,  $\gamma = 1/300$  day $^{-1}$ ,  $\delta = H_1/H_3 = 0.25$ . The restoring atmospheric temperatures are  $T_{1,2}^* = 22, 0^\circ\text{C}$ , and the freshwater (FW) forcing is  $FW_1 = -FW_2 = S_0 \times 100$  cm yr $^{-1} \times \text{Area}_1$ , with  $S_0 = 35$  ppt. The use of a linearized equation of state is a necessity because of the linear nature of the analysis to be applied below to this model, although it is may be expected to result in some bias because of the known stronger dependence of the density on salinity at low temperatures. The box model is very standard so we do not explore its parameter sensitivities here, which may be found, for example, in Griffies and Tziperman (1995), Tziperman et al. (1994), and Rivlin and Tziperman (1997).

### 3. Transient amplification and optimal initial conditions

Begin by examining the possibility of transient amplification of the THC by the nonnormal linearized dynamics in the linearly stable regime under mixed boundary conditions. Write the box model variables as steady-state solution plus a small perturbation,  $T_i = \bar{T}_i + T'_i$ . The equations for the temperature and salinity anomalies, linearized about the steady-state solution, in vector form, are

$$\begin{aligned}
 \frac{d\mathbf{P}}{dt} &= \mathbf{A}\mathbf{P} \\
 \mathbf{P} &\equiv [T'_1, T'_2, T'_3, S'_1, S'_2, S'_3], \quad (2)
 \end{aligned}$$

where  $\mathbf{A}$  is the  $6 \times 6$  matrix of the linearized model equations. Now drop the primes and consider the stability of the steady solution to small perturbations. Unlike the two-box Stommel (1961) model, the present model is characterized by a damped oscillatory behavior for FW forcing that is below some critical value (Tziperman et al. 1994). This oscillatory mode makes the dynamics richer and more interesting for the purpose of the following analysis.

The six eigenvectors  $\mathbf{e}_i$  and eigenvalues  $\lambda_i$  of the linearized model equations (Table 1) contain two rapidly decaying vectors with decay times in the order of 1–2 years that correspond to SST anomalies (vectors  $\mathbf{e}_1, \mathbf{e}_2$  in Table 1), two oscillatory (complex) modes with an oscillatory and decay times on the order of a few decades ( $\mathbf{e}_3, \mathbf{e}_4$ ), and a slowly decaying mode ( $\mathbf{e}_5$ ). Finally, there is one mode with a zero eigenvalue that corresponds to a constant shift in the salinity of all boxes ( $\mathbf{e}_6$ ), to which the THC is not sensitive, nor any of the other model equation (hence the zero eigenvalue).

We now wish to find the optimal initial conditions  $\mathbf{P}(t = 0)$  that maximize the THC at a time  $\tau$ ,  $U(t = \tau)^2$ . This measure to be maximized may be written as

$$J(\tau) \equiv \mathbf{P}(t = \tau)^T \mathbf{X} \mathbf{P}(t = \tau), \quad (3)$$

where

$$X_{ij} = R_i R_j \quad \mathbf{R} \cdot \mathbf{P} = U, \quad (4)$$

where  $\mathbf{R}$  is a six-dimensional vector that has the explicit form [derived from the first two equations in (1)]

$$\mathbf{R} = u_0 [\delta \alpha, -\alpha, (1 - \delta) \alpha, -\delta \beta, \beta, -(1 - \delta) \beta]. \quad (5)$$

TABLE 1. Eigenvectors and inverse eigenvalues of the linearized box model equations in a typical stable oscillatory regime. The inverse eigenvalues given in the top row of the table are in units of years.

	$\mathbf{e}_1$	$\mathbf{e}_2$	$\mathbf{e}_3$	$\mathbf{e}_4$	$\mathbf{e}_5$	$\mathbf{e}_6$
$\lambda^{-1}$	-0.6539	-0.8164	-80.8612 + $i$ 30.5346	-80.8612 - $i$ 30.5346	-135.3168	$\infty$
$T_1$	-0.6656	0.9523	0.2754 + 0.2904 <i>i</i>	0.2754 - 0.2904 <i>i</i>	-0.0925	-0.0000
$T_2$	0.7463	0.3052	-0.2693 - 0.2806 <i>i</i>	-0.2693 + 0.2806 <i>i</i>	0.1161	0.0000
$T_3$	-0.0041	-0.0021	-0.0627 + 0.0767 <i>i</i>	-0.0627 - 0.0767 <i>i</i>	0.9640	-0.0000
$S_1$	-0.0062	-0.0010	0.6526	0.6526	-0.2142	0.5774
$S_2$	0.0063	0.0010	-0.3194 - 0.3681 <i>i</i>	-0.3194 + 0.3681 <i>i</i>	0.0063	0.5774
$S_3$	-0.0000	-0.0000	-0.0833 + 0.0920 <i>i</i>	-0.0833 - 0.0920 <i>i</i>	0.0520	0.5774

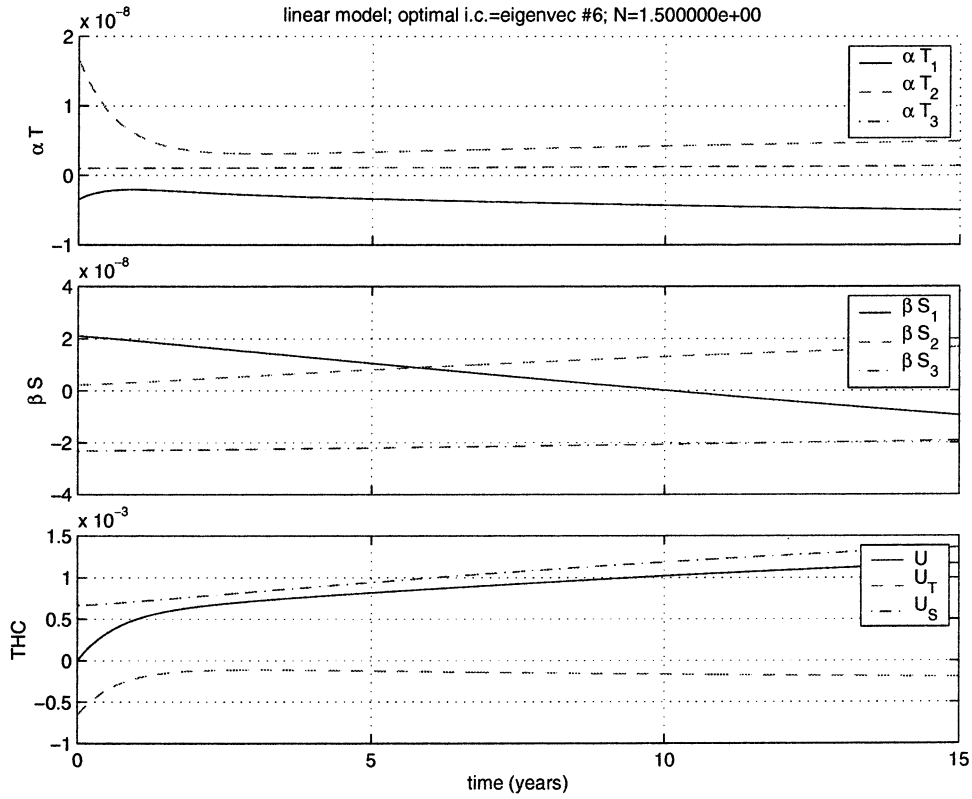


FIG. 2. THC anomaly calculated by the linearized model equations. Initial conditions are those that maximize the transient amplification of the THC anomaly at  $\tau = 2$  yr, according to mechanism 1 (see text): (top)  $\alpha T_i$ , (middle)  $\beta S_i$ , (bottom) THC and its temperature and salinity components.

The THC may be divided into the separate contributions of the temperature and the salinity:

$$\begin{aligned} U_T &= \mathbf{R}_T \cdot \mathbf{P} \\ U_S &= \mathbf{R}_S \cdot \mathbf{P} \\ \mathbf{R}_T &= u_0[\delta\alpha, -\alpha, (1 - \delta)\alpha, 0, 0, 0] \\ \mathbf{R}_S &= u_0[0, 0, 0, -\delta\beta, \beta, -(1 - \delta)\beta]. \end{aligned} \quad (6)$$

Note that the norm kernel  $\mathbf{X}$  is singular for the above norm that measures the THC amplitude (the rank of  $\mathbf{X}$  is one). The maximization is done subject to the condition that the initial conditions have a unit norm under some possibly different norm kernel  $\mathbf{Y}$ :

$$J(0) = \mathbf{P}(t=0)^T \mathbf{Y} \mathbf{P}(t=0) = 1. \quad (7)$$

Now, the solution to the model equation is

$$\mathbf{P}(t = \tau) = e^{\mathbf{A}\tau} \mathbf{P}(t = 0) = \mathbf{B}(\tau, 0) \mathbf{P}(t = 0), \quad (8)$$

where  $\mathbf{B}(t, s)$  is the propagator from time  $s$  to time  $t$ :  $\mathbf{P}(t) = \mathbf{B}(t, s) \mathbf{P}(s)$ . We wish to find the optimal initial conditions that maximize  $\mathbf{P}(t = \tau)^T \mathbf{X} \mathbf{P}(t = \tau)$  subject to  $\mathbf{P}(t = 0)^T \mathbf{Y} \mathbf{P}(t = 0) = 1$ . For this purpose, we need to solve the constrained optimization problem

$$\max_{\mathbf{P}_0} \{ \mathbf{P}_0^T \mathbf{B}^T \mathbf{X} \mathbf{B} \mathbf{P}_0 + \lambda \mathbf{P}_0^T \mathbf{Y} \mathbf{P}_0 \}, \quad (9)$$

where  $\mathbf{P}_0 = \mathbf{P}(t = 0)$ . By equating the derivative of this expression with respect to  $\mathbf{P}_0$  to zero, we find that the optimal initial conditions are the eigen vectors  $\mathbf{e}$  of the generalized eigen problem

$$\mathbf{B}(\tau, 0)^T \mathbf{X} \mathbf{B}(\tau, 0) \mathbf{e} = \lambda \mathbf{Y} \mathbf{e}. \quad (10)$$

Let us now set  $\mathbf{Y} = \mathbf{X}$  with  $\mathbf{X}$  from (4) reflecting the amplitude of the THC. Because  $\mathbf{X}$  is singular, the eigen problem (10) is singular. We therefore need to regularize  $\mathbf{X}$  as explained in the appendix. In this case, the eigen vector  $\mathbf{e}_1$ , with the largest eigenvalue of (10) is the spatial structure of the normalized temperature and salinity initial conditions that results in the largest THC amplification at a time  $\tau$ . The actual amplification of the THC in this case is the corresponding eigenvalue  $\lambda$ . By examining the optimal transient amplification for a variety of run times  $\tau$ , we find that there are two different physical mechanisms that allow for transient amplification of the THC in the box model. One has a typical timescale of  $O(2)$  years and the other  $O(40)$  years. We now consider each of these in some detail.

Figure 2 shows the temperature, salinity, and THC calculated by the linearized model as function of time for the optimal initial conditions obtained with an optimization time  $\tau = 2$  yr. The solid line in the lower panel of that figure shows that the optimal initial con-

ditions correspond to a zero value of the initial THC, and to a rapid growth within a timescale of some 2–3 years. (At that stage the THC starts to slowly increase as part of a slow oscillation due to the oscillatory modes of the model dynamics.) The physical interpretation of the rapid initial growth is very simple. The initial THC anomaly depends on both the temperature and salinity distributions. The dash and dash–dot lines in the lower panel of Fig. 2 show that the transient amplification of the THC is due to the interaction of the rapidly decaying SST modes and the slow-decaying oscillatory modes. In mathematical terms, these modes are nonorthogonal in the norm whose kernel is  $\mathbf{X}$ . In more physical terms, we note that the initial conditions correspond to temperature and salinity perturbations that create exactly canceling contributions to the THC,  $U_T = -U_S$  (6), so that the THC anomaly vanishes at  $t = 0$ ,  $U(t = 0) = 0$ . The THC due to the temperature perturbations,  $U_T$ , depends mostly on the surface temperature in this optimal mode, and therefore decays rapidly to zero, causing the total THC to rapidly grow to the value of the much slower decaying salinity contribution  $U_S$ .

This transient amplification mechanism due to the interaction of two (or more) nonorthogonal eigenmodes with different decay times is typical of nonnormal systems (Farrell and Ioannou 1996). Typically in such systems optimal small-amplitude initial conditions are the superposition of two (nonorthogonal) large-amplitude eigenmodes of the system. The two large-amplitude components composing the initial conditions partially cancel each other, resulting in a small-amplitude initial condition. One of these eigenmodes has a rapid decay time, while the other a slower decay time. After some short time past the initial conditions, the faster-decaying eigenmode vanishes, leaving only the component of the initial conditions corresponding to the slowly decaying eigenmode. This decay eliminates the mutual cancellation between the two modes, and the system finds itself at a state that is close to the large initial value of the slower-decaying mode, hence the initial amplification. At a later time the remaining eigenmode slowly decays to zero as well.

Note that because the initial THC anomaly vanishes for the optimal initial conditions, whose time evolution is plotted in Fig. 2, the actual amplification  $U(\tau)/U(0)$  is infinite, and so is the eigenvalue corresponding to this mode. (As explained in the appendix, when the norm Kernel  $\mathbf{X}$  is regularized, the initial THC approaches zero, and the amplification approaches infinity, as the regularization constant  $\varepsilon$  approaches zero.) Although the amplification relative to the initial value of the THC is infinite, the actual maximal value of the THC depends on the amplitude of the initial salinity perturbations. The eventual maximum amplitude to which the THC anomaly may reach is limited by the initial amplitude of the salinity contribution to the THC,  $U_S$ .

This brings us to one of the two motivations for this study mentioned in the introduction. That is, can a tran-

sient amplification of small-amplitude initial perturbation to the ocean state cause a large-amplitude transient amplification that would bring the THC below the stability threshold? It seems from the above discussion that this is not likely to happen, as the eventual amplitude of the THC anomaly at the maximum transient amplification is limited by the contribution of the salinity anomalies of the initial conditions to the THC. Thus to get a large THC amplification, we need a large initial salinity anomaly, not a small one.

The second physical mechanism of transient THC growth is shown in Fig. 3 and is different from the one described above in several aspects. First, it occurs after a time of  $O(40)$  years, rather than a couple of years as in the first mechanism. Second, it involves mostly a slow reorganization of the salinity and temperature anomalies in the model, rather than an interaction of the fast decaying temperature modes and slow salinity modes as discussed above. As can be seen in the lower panel of Fig. 3, the contribution of the temperature ( $U_T$ , dash) to the changes in the THC anomaly (solid) is negligible, and the THC anomaly due to salinity anomalies ( $U_S$ , dash–dot) dominates throughout the shown time series. The spatial structure of the optimal initial conditions is such that the initial THC is very close to zero separately for both the temperature and the salinity contributions (the two still cancel at  $t = 0$ , so that  $U_S = -U_T$ ). Note that this is distinctly different from the first mechanism discussed above. However, as the salinity anomalies evolve in time because of both the advection of the anomalies by the mean THC and the advection of the mean salinity gradients by the anomalous THC, the structure of the salinity anomalies at a time of 40 yr past the initial conditions evolves into a structure that maximizes the salinity contribution to the THC,  $U_S$ . This basically happens because of the evolution of the southern surface box salinity  $S_1$  and the polar box salinity  $S_2$  as can be seen in the middle panel of Fig. 3. Note again that while changes do occur in the temperature field (upper panel), they are of little consequence to the evolution and transient growth of the THC (dashed line, lower panel of Fig. 3). Unlike in the first mechanism discussed above, the second mechanism relies mostly on the slower-decaying eigenmodes of the linearized model matrix. Because of the timescales of these modes (see  $\mathbf{e}_3$ ,  $\mathbf{e}_4$ ,  $\mathbf{e}_5$  in Table 1) are different by only a factor of 2 from each other, the transient amplification is not very rapid relative to the eventual decay timescales (as explained above, the transient amplification typically has the timescale of the fastest decaying relevant eigenmode, and the perturbation then decays according to the timescale of the slowest decaying mode, (Farrell and Ioannou 1996). Moreover, it should be quite clear from Fig. 3 that the second “amplification” mechanism is not very different from the oscillatory mechanism of the two complex oscillatory modes seen in Table 1. Such oscillatory modes always have phases with a zero value of the THC that later develop into a nonzero THC. To

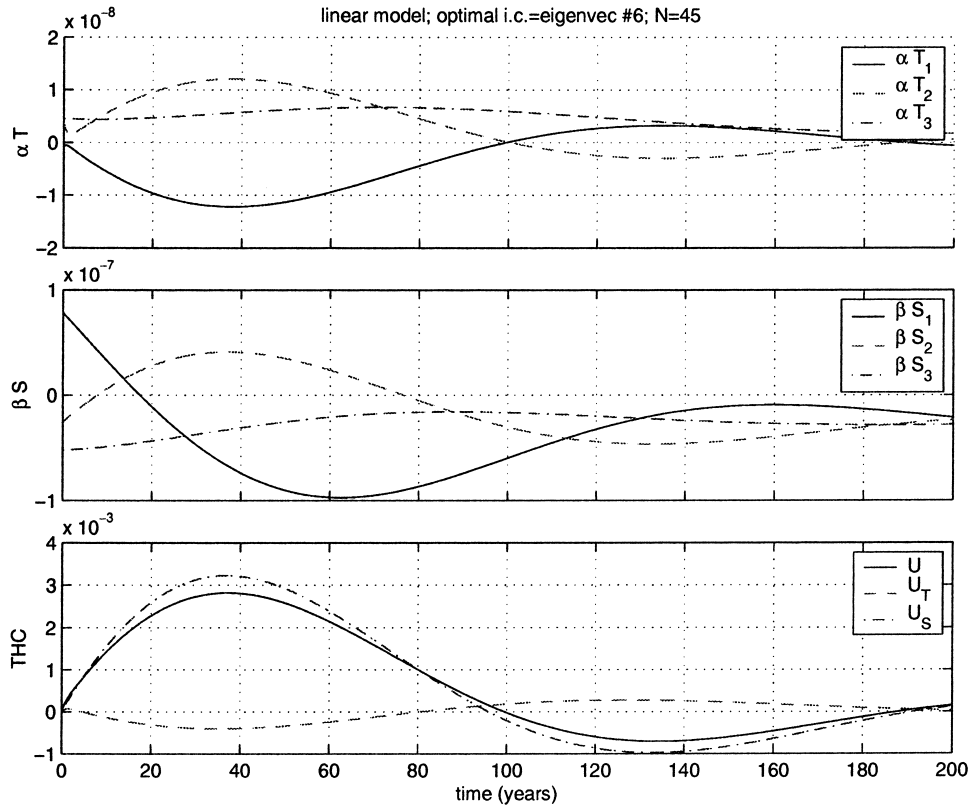


FIG. 3. THC anomaly calculated by the linearized model equations. Initial conditions are those that maximize the transient amplification of the THC anomaly at  $\tau = 45$  yr, according to mechanism 2 (see text): (top)  $\alpha T_i$ , (middle)  $\beta S_i$ , (bottom) THC and its temperature and salinity components.

some degree, that is what happens in the above second growth mechanism, although some other nonoscillatory modes of the linearized model also contribute to the optimal initial conditions of this second transient amplification mechanism.

It might be useful to add a word regarding the norm kernel  $\mathbf{X}$  used here. In works looking at the nonnormal transient amplification in various models, one normally makes an effort to show that the results do not depend on the choice of norm. It is important to understand that in the present work, we are interested particularly in the specific norm used here which measures the amplification of the THC. Using an energy norm, for example (sum of squares of the temperature and salinity), may eliminate the interesting growth mechanisms explored here, and would simply be irrelevant to the objective of this work, which has to do with transient amplification of the THC itself. It is possible that a norm kernel  $\mathbf{X}$  which measures the THC amplitude in a more realistic model may not be singular. However, the two specific physical mechanisms found here using the singular norm kernel are physically sensible and therefore should be robust in fuller models as well.

Having identified two physical mechanisms for transient THC amplification, we now proceed to study the

optimal excitation of the THC by continuous stochastic forcing.

#### 4. Stochastic optimals

Consider now a white noise heat and freshwater forcing of the THC added to the mean surface forcing fields. In this case we would like to know what is the optimal spatial structure (stochastic optimals) of the noise that results in maximal variance of the THC variability. The derivation below follows Kleeman and Moore (1997) and is also practically identical to that of Farrell and Ioannou (1996). The forced linearized model equation is

$$\dot{\mathbf{P}} = \mathbf{A}\mathbf{P} + \mathbf{F}\mathbf{f}(t), \tag{11}$$

where  $\mathbf{f}$  is a six-vector noise forcing term and  $\mathbf{F}$  is a matrix operator restricting the noise to the surface boxes only (boxes 1 and 2):  $F_{ij} = 1$  for  $i = j = 1, 2, 4, 5$  and  $F_{ij} = 0$  elsewhere. The solution to the model equation (11) is

$$\begin{aligned} \mathbf{P}(\tau) &= e^{\mathbf{A}\tau}\mathbf{P}(0) + \int_0^\tau ds e^{\mathbf{A}(\tau-s)}\mathbf{F}\mathbf{f}(s) \\ &= \mathbf{B}(\tau, 0)\mathbf{P}(0) + \int_0^\tau ds \mathbf{B}(\tau, s)\mathbf{F}\mathbf{f}(s). \end{aligned} \tag{12}$$

We are interested in the variance of the THC defined using the norm kernel  $\mathbf{X}$ :

$$\text{Var}(\|\mathbf{P}\|) \equiv \langle P_i(\tau)X_{ij}P_j(\tau) \rangle - \langle P_i(\tau) \rangle X_{ij} \langle P_j(\tau) \rangle,$$

where the average  $\langle \rangle$  is over realizations of the noise  $\mathbf{f}$ . Based on the solution (12) for  $\mathbf{P}$ , we have  $\langle P_i(\tau) \rangle = \langle B_{ij}(\tau, 0)P_j(0) \rangle$  so that

$$\begin{aligned} \text{Var}(\|\mathbf{P}\|) &= \left\langle \int_0^\tau ds \int_0^\tau dt B_{il}(\tau, s) F_{l'l'} f_{l'}(s) X_{ij} B_{jn}(\tau, t) \right. \\ &\quad \left. \times F_{m'n'} f_{n'}(t) \right\rangle \\ &= \int_0^\tau ds \int_0^\tau dt B_{il}(\tau, s) X_{ij} B_{jn}(\tau, t) F_{l'l'} F_{m'n'} \\ &\quad \times \langle f_{l'}(s) f_{n'}(t) \rangle, \end{aligned} \quad (13)$$

specifying the noise statistics to be separable in space and time,

$$\langle f_{l'}(t) f_{n'}(s) \rangle = C_{l'n'} D(t - s),$$

we have

$$\begin{aligned} \text{Var}(\|\mathbf{P}\|) &= \int_0^\tau ds \int_0^\tau dt B_{il}(\tau, s) F_{l'l'} X_{ij} B_{jn}(\tau, t) \\ &\quad \times F_{m'n'} C_{l'n'} D(t - s) \\ &= \text{Tr} \left\{ \left[ \int_0^\tau ds \int_0^\tau dt D(t - s) \mathbf{F}^\top \mathbf{B}(\tau, s) \right]^\top \right. \\ &\quad \left. \times \mathbf{X} \mathbf{B}(\tau, t) \mathbf{F} \right] \mathbf{C} \} \\ &= \text{Tr}[\mathbf{Z}\mathbf{C}]. \end{aligned} \quad (14)$$

With this last expression we can now calculate the stochastic optimals, that are the eigenvectors of  $\mathbf{Z}$  with the largest eigenvalues (Farrell and Ioannou 1996; Kleeman and Moore 1997). The actual computational examples below are worked out with the noise  $f_n$  at any given spatial location and time step  $n$  being a 1D Markov process:

$$\begin{aligned} f_{n+1} &= Rf_n + \sqrt{1 - R^2} v_n \\ R &\equiv \exp(-\Delta t/T_{\text{corr}}) \\ \langle v_n v_m \rangle &\equiv \sigma^2 \delta_{nm} \\ D(t_n - t_m) &\equiv \langle f_{n+m} f_n \rangle \\ &= \sigma^2 e^{-m\Delta t/T_{\text{corr}}}. \end{aligned} \quad (15)$$

The matrix  $\mathbf{Z}$  is evaluated from the double time integral of (14) by changing variables of integration to  $r = t - s$ ;  $q = t + s$  such that  $s = (q - r)/2$ ;  $t = (q + r)/2$ . Note that the coordinate transformation may be written using a  $2 \times 2$  matrix  $\mathbf{M}$  as  $(r, q) = \mathbf{M}(t, s)$  where  $\mathbf{M} = [1, -1; 1, 1]$  so that  $dt ds = \det(\mathbf{M}^{-1}) dr dq = (1/2) dr$

$dq$ . For efficiency, truncate integration region in the  $(r, q)$  plane to  $|r| = |t - s| < T_{\text{trunc}} \ll \tau$ , which would be a good approximation as long as  $T_{\text{trunc}} \gg T_{\text{corr}}$ , due to the short correlation time of the noise as expressed in the  $D(t - s) = D(r)$  factor in (15). Note also that the matrix  $\mathbf{Z}$  is independent of the time  $\tau$  as long as it is sufficiently longer than the relevant physical decay times of the model (the neutral mode with infinite decay time of our linearized equations does not affect the THC, so the time  $\tau$  needs to be a few times the slowest decay time seen in Table 1).

Figure 4 shows time series of the temperature, salinity, and THC from the solution of the linearized box model (2) forced by stochastic noise in the heat and freshwater fluxes that has the spatial structure obtained from the most optimal eigenvector of  $\mathbf{Z}$  ( $\mathbf{f}_6$ , Table 2). Similarly, Fig. 5 shows the results when forcing by the third most optimal such eigenvector ( $\mathbf{f}_4$ ). Clearly the solution forced by the first eigenvector has a larger variance of the THC, as expected given the norm  $\mathbf{X}$  we are using. This can also be seen in the spectra of the THC time series forced by the different eigenvectors of  $\mathbf{Z}$ , shown in Fig. 6. Note that not only the variance is different, but also the less optimal modes produce higher-frequency response. It seems that the most optimal two eigenvectors ( $\mathbf{f}_{5,6}$  in Table 2) excite mostly the salinity-controlled THC variability modes, while the less optimal eigenvectors excite the thermally controlled variability modes (compare  $U_T$  and  $U_S$  in the lower panel of Figs. 4 and 5). This is also seen in Table 2 which shows the spatial structure of the stochastic optimals, and the corresponding eigenvalues which reflect the degree of excitability of each mode (Kleeman and Moore 1997; Farrell and Ioannou 1996).

The spectra of the model solution for the THC (Fig. 6) is basically red, with no large-amplitude peaks. The model does have an oscillatory mode that may be excited to produce a peak at the appropriate period of about thirty years (see complex eigenvalues in Table 1). However, there is also an exponentially decaying mode that is slower decaying than the oscillatory damped modes, and it seems that the excitation of this mode dominates, resulting in no large spectral peaks at the frequency of the oscillatory modes in the stochastically forced model solution.

There is one issue we need to be aware of regarding stochastically forcing the salinity in ocean models such as the one used here. Because there is a zero mode of the box model corresponding to a constant shift in the salinities of all boxes ( $\mathbf{e}_6$  in Table 1), the ensemble average salinity variance can grow indefinitely and linearly in time when forced with uncorrelated freshwater forcing. This can be seen in the slow drift of the mean salinity seen in the middle panel of Fig. 4. In reality, this drift of the mean salinities is limited by the finite mass of the freshwater available for evaporation ( $E$ ) minus precipitation ( $P$ ) (mostly due to the finite mass of land glaciers whose accumulation and melting pro-

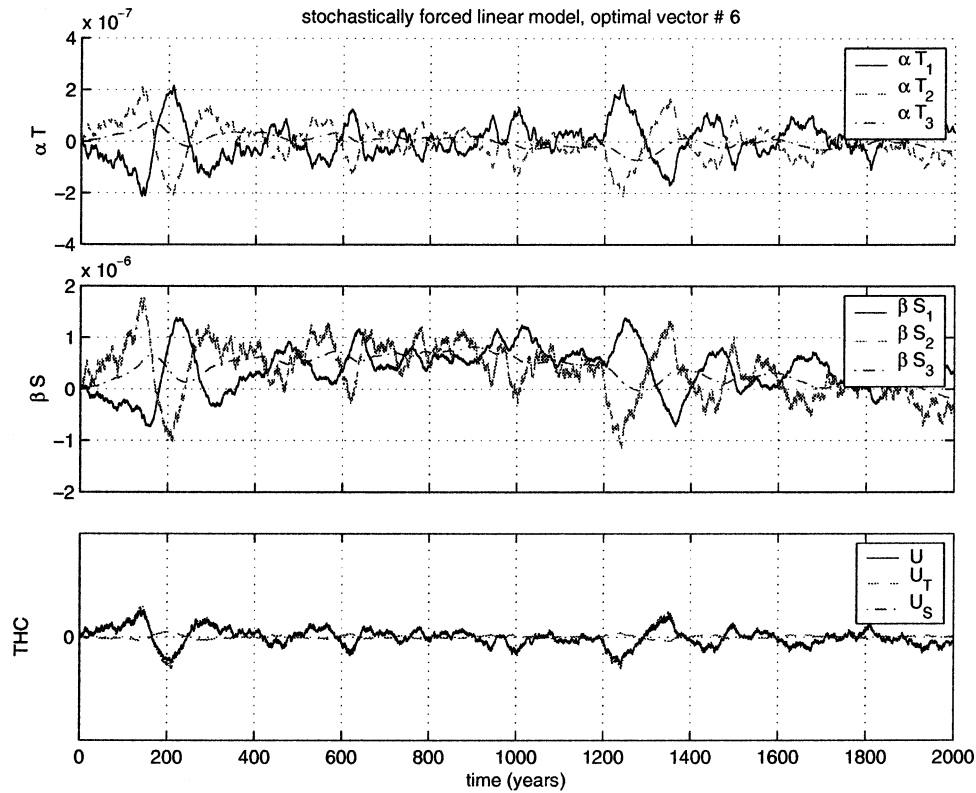


FIG. 4. Response of the linearized box model THC to stochastic surface forcing patterns based on the most optimal eigenvector of  $\mathbf{Z}$ : (top)  $\alpha T_i$  for all boxes, as function of time; (middle)  $\beta S_i$ , (bottom) the THC anomaly, as well as its temperature and salinity components,  $U_T$  and  $U_S$ .

vide the sink/source for the net freshwater flux into the ocean). This implies that in order to prevent the variance of salinity perturbations in the ocean from growing indefinitely, we should actually use a FW flux that is constrained by an explicit glacier mass balance equation. Such FW forcing will be characterized by long time correlations corresponding to the timescale of the land glaciers ( $\tau_G \sim$  tens of thousands of years). Alternatively, we can consider only timescales that are significantly smaller than  $\tau_G$ . On such timescales, shorter than the time it takes for the finite mass of the glaciers to have an effect, it is realistic to expect the averaged salinity variance to grow linearly in time. Note that alternatively, we could have demanded that the net  $E - P$  forcing of the ocean box model vanishes, basically

demanding that precipitation over the high-latitude ocean at any given time only comes from the instantaneous evaporation from the ocean over the lower latitudes. However, this is not a physically realistic constraint, because the land glaciers can provide a net sink/source making the net  $E - P$  nonzero at any given moment. Note that, in any case, because there are only two surface boxes in this model, adding a constraint of zero net  $E - P$  at any given time would mean that the spatial structure of the noise is determined completely. There would, of course, be no meaning to a calculation of the optimal spatial structure of the stochastic forcing then.

**5. Conclusions**

We have examined the optimal initial conditions that lead to transient growth of THC anomalies in a simple meridional box model. The possible physical mechanisms that lead to such transient growth were analyzed in some detail. One such mechanism is based on an interaction of the thermally driven and salinity-driven components of the THC anomalies. We found that initially, the two components exactly balance in the optimal initial conditions, leading to a zero initial value of the THC anomaly. The thermal component then de-

TABLE 2. Eigenvectors (stochastic optimals) and eigenvalues of the matrix  $\mathbf{Z}$ .

	$\mathbf{f}_1$	$\mathbf{f}_2$	$\mathbf{f}_3$	$\mathbf{f}_4$	$\mathbf{f}_5$	$\mathbf{f}_6$
$\lambda$	0	0	0	0.001	0.452	2.567
$T_1$	0	0	-0.9824	-0.1862	-0.0033	0.0015
$T_2$	0	0	-0.1862	0.9822	0.0220	-0.0066
$T_3$	-1	0	-0.0000	0.0000	0.0000	0.0000
$S_1$	0	0	0.0008	-0.0190	0.9491	0.3142
$S_2$	0	0	-0.0000	0.0135	-0.3140	0.9493
$S_3$	0	1	0	0	0	0

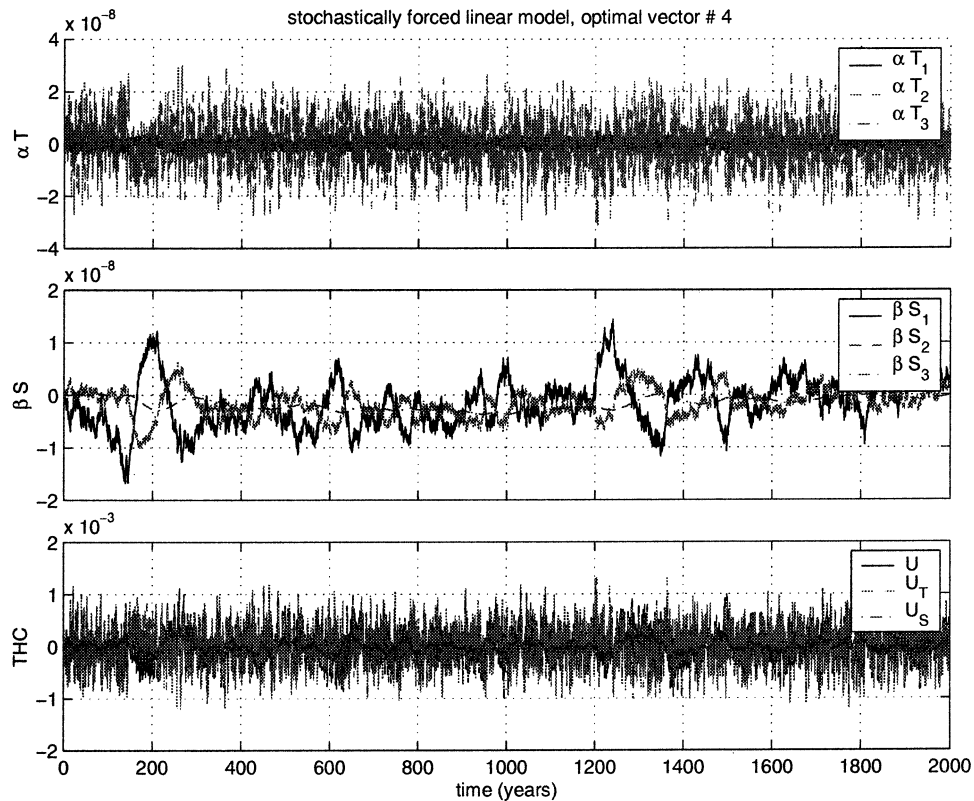


FIG. 5. Same as Fig. 4, but for third optimal eigenvector of  $\mathbf{Z}$ .

cays rapidly (within a couple of years or so) because of the restoring thermal boundary conditions, making the THC anomaly grow to the initial value of the salinity-driven THC anomaly component. The second transient growth mechanism involves a rearrangement of the initial salinity anomaly field that leads to the growth of the THC anomaly. This second mechanism is closely related to the oscillatory modes of the linearized model dynamics.

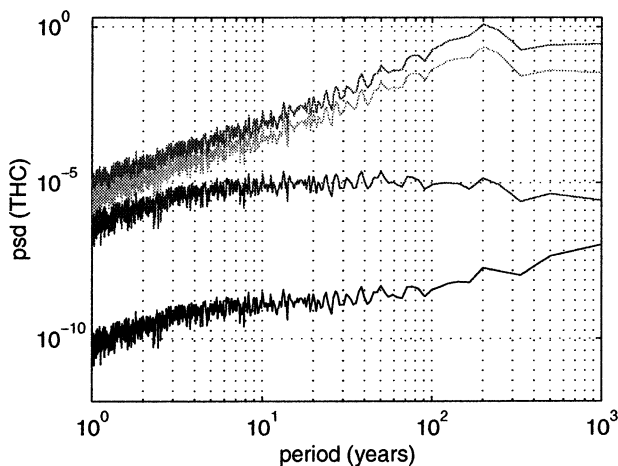


FIG. 6. Power spectral density of the time series of the THC in the box model forced by the four stochastic optimals  $\mathbf{f}_{3,4,5,6}$ .

The optimal stochastic atmospheric forcing of heat and freshwater fluxes were also calculated. It was shown that the optimal forcing induces low-frequency variability by exciting the salinity variability modes of the THC.

There are some very basic questions that we have not been able to address here: What is the concert physical meaning of the ordinary and stochastic optimals? How could such perturbations actually be realized? Do observations project into these optimal modes? These three important questions are ones that have been answered very nicely in the context of the optimal excitation of ENSO, where the observed westerly wind bursts seem similar to the optimal forcing calculated by some models (Moore and Kleeman 1999). This situation is more difficult to reproduce presently in the context of the THC. With the two-point resolution in space in the box model used here for an entire ocean basin, it is difficult to compare calculated optimal surface forcing patterns with observations. Once the same analysis is done with a fuller-resolution model, it would hopefully be possible to analyze the available observations of air-sea fluxes and look for modes that project on the optimal stochastic forcing.

It is quite satisfactory that we have been able to identify two simple physical mechanisms that can result in transient THC amplification, as well as get some physical intuition into the mechanism of optimal stochastic

forcing of the THC by stochastic atmospheric heat and freshwater forcing. Past experience with THC box models has proven that when a physical mechanism can be identified in such simple models, it is more often than not also found in fuller and more complex/realistic models. One example out of many possible ones is the conjecture of Walin (1985) and Tziperman et al. (1994) based on simple box models, that present-day climate might be close to a stability threshold, which has later found additional evidence in the ocean and coupled GCM studies of Tziperman et al. (1994) and Tziperman (1997). It would clearly be interesting therefore to examine the findings here in fuller models of the THC. Such an examination using fuller models is obviously necessary to evaluate the relevance of the findings here to the actual THC.

*Acknowledgments.* Many thanks to Paola Cessi and Eli Galanti for most useful discussions during this work, and to two anonymous reviewers for their constructive and knowledgeable comments.

#### APPENDIX

##### Transient Growth Using a Singular Norm Kernel

Solving the eigen problem (10) with singular norm kernel may lead to an infinite amplification factor with optimal modes for which the initial value of the THC is zero and the value at the optimization time is finite. Now, if there are two or more such eigenmodes, they may be linearly superimposed resulting again in a mode with infinite amplification factor. This nonuniqueness of the optimal eigenmodes may result in a suboptimal transient growth estimate. It is therefore necessary to regularize the eigen problem by adding a small diagonal matrix to the norm kernel

$$\mathbf{X}_\varepsilon = \mathbf{X} + \varepsilon \mathbf{I}.$$

We have therefore used  $\mathbf{X} = \mathbf{Y} = \mathbf{X}_\varepsilon$  in (10). Once this is done, the initial THC value for the optimal mode is not zero, and the optimal amplification factor is not infinite but tends to infinity as  $\varepsilon$  approaches zero.

#### REFERENCES

- Cessi, P., 1994: A simple box model of stochastically forced thermohaline flow. *J. Phys. Oceanogr.*, **24**, 1911–1920.
- Chen, F., and M. Ghil, 1995: Interdecadal variability of the thermohaline circulation and high-latitude surface fluxes. *J. Phys. Oceanogr.*, **25**, 2547–2568.
- Delworth, T., S. Manabe, and R. J. Stouffer, 1993: Interdecadal variations of the thermohaline circulation in a coupled ocean–atmosphere model. *J. Climate*, **6**, 1993–2011.
- Farrell, B., 1988: Optimal excitation of neutral Rossby waves. *J. Atmos. Sci.*, **45**, 163–172.
- , and P. J. Ioannou, 1996: Generalized stability theory. Part I: Autonomous operators. *J. Atmos. Sci.*, **53**, 2025–2040.
- Griffies, S. M., and E. Tziperman, 1995: A linear thermohaline oscillator driven by stochastic atmospheric forcing. *J. Climate*, **8**, 2440–2453.
- Kleeman, R., and A. M. Moore, 1997: A theory for the limitation of ENSO predictability due to stochastic atmospheric transients. *J. Atmos. Sci.*, **54**, 753–767.
- Moore, A. M., and R. Kleeman, 1999: Stochastic forcing of ENSO by the intraseasonal oscillation. *J. Climate*, **12**, 1199–1220.
- Rivlin, I., and E. Tziperman, 1997: Linear versus self-sustained interdecadal thermohaline variability in a coupled box model. *J. Phys. Oceanogr.*, **27**, 1216–1232.
- Stommel, H., 1961: Thermohaline convection with two stable regimes of flow. *Tellus*, **13**, 224–230.
- Tziperman, E., 1997: Inherently unstable climate behaviour due to weak thermohaline ocean circulation. *Nature*, **386**, 592–595.
- , J. R. Toggweiler, Y. Feliks, and K. Bryan, 1994: Instability of the thermohaline circulation with respect to mixed boundary-conditions: Is it really a problem for realistic models? *J. Phys. Oceanogr.*, **24**, 217–232.
- Walin, G., 1985: The thermohaline circulation and the control of ice ages. *Paleogeogr. Paleoclimatol. Paleoecol.*, **50**, 323–332.
- Weaver, A. J., E. S. Sarachik, and J. Marotzke, 1991: Freshwater flux forcing of decadal and interdecadal oceanic variability. *Nature*, **353**, 836–838.
- Winton, M., and E. S. Sarachik, 1993: Thermohaline oscillation induced by strong steady salinity forcing of ocean general circulation models. *J. Phys. Oceanogr.*, **23**, 1389–1410.